Journal of Environmental Quality SPECIAL SECTION

ENVIRONMENTAL BENEFITS OF BIOCHAR

Macroscopic and Molecular Investigations of Copper Sorption by a Steam-Activated Biochar

J. A. Ippolito,* D. G. Strawn, K. G. Scheckel, J. M. Novak, M. Ahmedna, and M. A. S. Niandou

Excessive Cu concentrations in water systems can negatively affect biological systems. Because Cu can form strong associations with organic functional groups, we examined the ability of biochar (an O-C–enriched organic bioenergy by-product) to sorb Cu from solution. In a batch experiment, KOH steam–activated pecan shell biochar was shaken for 24 h in pH 6, 7, 8, or 9 buffered solutions containing various Cu concentrations to identify the effect of pH on biochar Cu sorption. Afterward, all biochar solids from the 24-h shaking period were air-dried and analyzed using X-ray absorption fine structure (XAFS) spectroscopy to determine solid-phase Cu speciation. In a separate batch experiment, biochar was shaken for 30 d in pH 6 buffered solution containing increasing Cu concentrations; the Cu sorption maximum was calculated based on the exponential rise to a maximum equation. Biochar sorbed increasing amounts of Cu as the solution pH decreased from 9 to 6. The XAFS spectroscopy revealed that Cu was predominantly sorbed onto a biochar organic phase at pH 6 in a molecular structure similar to Cu adsorbed on model humic acid (Cu–humic acid [HA]). The XAFS spectra at pH 7, 8, and 9 suggested that Cu was associated with the biochar as three phases: (i) a complex adsorbed on organic ligands similar to Cu-HA, (ii) carbonate phases similar to azurite ($Cu_3(CO_3)_2(OH_2)$), and (iii) a Cu oxide phase like tenorite (CuO). The exponential rise equation fit to the incubated samples predicted a Cu sorption maximum of 42,300 mg Cu kg^{-1}. The results showed that KOH steam–activated pecan shell biochar could be used as a material for sorbing excess Cu from water systems, potentially reducing the negative effects of Cu in the environment.

J. Environ. Qual. 41
doi:10.2134/jeq2011.0113
Supplemental data file is available online for this article.
Received 30 Mar. 2011.
*Corresponding author (jim.ippolito@ars.usda.gov).
© ASA, CSSA, SSSA
5585 Guilford Rd., Madison, WI 53711 USA

Copper is an essential element, but elevated concentrations in soils, waters, and wastewaters can be toxic to the environment. One potential source of Cu to the environment comes from dairy operations that use hoofbaths containing Cu concentrations between 12,500 and 25,000 mg L^{-1} to control hoof diseases (Stehouwer and Roth, 2009). Hoofbath solution is typically released into liquid waste lagoons (Ippolito et al., 2010), with lagoon water eventually being used for crop irrigation. Here, environmental degradation can be realized. Thus, removing Cu from the spent hoofbath before release into the waste lagoon could lessen the environmental impact of Cu-laden dairy lagoon wastewaters.

Conventional methods of Cu removal from waste streams are precipitation, ion exchange, electrolysis, and adsorption onto activated carbon (Özer et al., 2004). However, these processes create operative issues because they are expensive to install or sophisticated to operate. As an alternative to these issues, ideal materials for sorbing Cu from waters could be low-cost organic by-products or waste materials from another industry (Low et al., 2000) that otherwise would be disposed of but that can sequester Cu because Cu forms strong associations with organic phases (e.g., Kalis et al., 2006; Rodriguez-Rubio et al., 2003; McBride and Blasiak, 1979).

Charcoal has a long history of serving as an efficient filter media for removing impurities from aqueous systems. More recently, biochar, an organic by-product from bioenergy production, has been used as a media for sorption of heavy metals from soils and industrial wastes (Beesley et al., 2010; Uchimiya et al., 2010b). Biochar is relatively recalcitrant as compared with other organic wastes (e.g., manures, composts, green manures, or biosolids) and therefore could possibly supply a long-term means of sorbing excess Cu from the environment. With respect to Cu sorption, several researchers have shown mixed results using biochars in composts and soils.

Hua et al. (2009) composted biosolids and rapeseed (*Brassica napus* L.) made with up to 9% (by weight) bamboo

---

J.A. Ippolito, USDA–ARS, Northwest Irrigation and Soils Research Lab., 3793 N. 3600E, Kimberly, ID 83341; D.G. Strawn, Dep. of Plant, Soil, and Entomological Sciences, Univ. of Idaho, College of Agricultural and Life Sciences, P.O. Box 442339, Moscow, ID 83844-2339; K.G. Scheckel, National Risk Management Research Lab., U.S. Environmental Protection Agency, 5995 Center Hill Ave., Cincinnati, OH 45224; J.M. Novak, USDA–ARS, Coastal Plains Research Center, Florence, SC 29501; M. Ahmedna and M.A.S. Niandou, Dep. of Human Environment and Family Sciences, North Carolina A&T Univ., Greensboro, NC 27411. Assigned to Associate Editor Géraldine Sarret.

Abbreviations: DTPA, diethylenetriaminepentaacetic acid; EXAFS, extended X-ray absorption fine structure; FT, Fourier transforms; HA, humic acid; LCF, linear combination fitting; XAFS, X-ray absorption fine structure; XANES, X-ray absorption near-edge structure.

biochar (pyrolyzed at 600°C). Biochar application reduced diethylenetriaminepentaacetic acid (DTPA)-extractable Cu by 44% as compared with the amount of extractable Cu before biochar usage. Additionally, they reported that DTPA-extractable Cu was 28% lower after composting with biochar as compared with treatments without biochars. Uchimiya et al. (2010b) researched soil Cu immobilization by poultry (*Gallus gallus* domesticus) broiler litter manure pyrolyzed at 350 and 700°C with or without steam activation. Poultry litter biochar was mixed at 10% by weight into a San Joaquin standard soil (NIST; Abruptic Durixeralfs) and shaken for 24 h in synthetic acid rain water (pH 4.5) containing 95 mg Cu L^{-1}. Soluble Cu concentrations for the 350°C with steam activation and the 700°C with or without steam activation were reduced to <1 mg L^{-1}. However, the authors observed a greater soluble Cu concentration (~10 mg L^{-1}) with the 350°C without steam activation treatment, which could have been due to Cu mobilization through chelation by soluble organic functional groups. Beesley et al. (2010) added 200 mL of hardwood-derived biochar pyrolyzed at 400°C to 400 mL of soil containing elevated metals, including Cu, and leached the mixture at 7, 14, 28, and 56 d. In contrast to the findings of Uchimiya et al. (2010b), biochar addition increased leachate Cu due to the biochar containing elevated Cu (70 mg kg^{-1}) (Hartley et al., 2009) or Cu-associated with dissolved organic C functional groups. In support of the latter finding, the authors observed a decrease in leachate Cu concentration over time corresponding to a dissolved organic C concentration decline.

Although the use of biochar to immobilize Cu in soils has had mixed success, biochar use for sorbing solution-borne Cu appears more promising. Hua et al. (2009) tested the ability of bamboo biochar to retain Cu from solution by mixing between 20 and 200 mmol Cu g^{-1} biochar and shaking for 48 h. Copper sorption ranged from 18 to 38% of the initial solution concentration and decreased with increasing adsorbate loading. This was speculated to be due to saturation of high-affinity binding sites on biochar. These researchers were also concerned about potential hysteresis effects, so biochar particles were separated and experiments were conducted to desorb Cu from particles using DTPA. Some hysteresis occurred, but the biochar retained between 74 and 88% of the original sorbed Cu. The strong Cu binding was likely due to robust covalent bonding between biochar functional groups and Cu. Uchimiya et al. (2010a) researched Cu immobilization in water by poultry broiler litter manure pyrolyzed at 350 and 700°C with or without steam activation. Using standard isotherm methods, 5 g of biochar L^{-1} were equilibrated for 24 h with 95 mg Cu L^{-1}. Equilibrium Cu concentrations decreased to approximately 32 and 13 mg L^{-1} without, and to approximately 2.5 and 3.2 mg L^{-1} with, the steam activation for the 350 and 700°C biochars, respectively. Greater Cu removal was caused by the biochar having its surface modified by creating more surface area due to higher pyrolysis temperatures and steam activation. Lima and Marshall (2005b) studied Cu sorption onto pelletized biochar made from poultry broiler litter and poultry cake. Pellets were pyrolyzed at 700°C and steam activated at 800°C. Copper sorption was then examined in standard isotherms by mixing 0.25 g biochar with 25 mL of 20 mmol L^{-1} $CuCl_2{\cdot}2H_2O$ solution. After 24 h, Cu sorption was 95 and 70% for the broiler cake and litter biochars, respectively. Unlike the Uchimiya et al. (2010a) results, greater pyrolysis activation times or steam flow produced biochars that caused reduced Cu sorption. In a similar study using biochars made from turkey (*Meleagris gallopavo*) litter–derived and manure-derived biochar, Lima and Marshall (2005c) showed that the greatest Cu sorption (93%) was obtained when the biochar was activated under a specific steam flow rate. These conditions optimized biochar performance in terms of yield, surface area, and Cu sorption. These results show that biochar's ability to sorb Cu is promising; however, its success depends on conditions used during the pyrolysis and activation phases of its manufacturer.

Understanding the Cu binding process with organic phases is important to develop better environmental models of biological or sediment Cu uptake and release. This is especially true regarding Cu binding from spent hoofbaths. Although some studies have analyzed speciation of Cu sorbed on organic materials (Xia et al., 1997; Karlsson et al., 2006; Strawn and Baker, 2009; Manceau and Matynia, 2010), there have been no molecular-scale investigations of Cu sorption on biochar. Information on Cu-binding mechanisms can be ascertained in Cu sorption experiments using X-ray absorption fine structure (XAFS) spectroscopy. Therefore, the objectives of this work were to identify adsorption behavior of solution-borne Cu on KOH-activated pecan shell–based biochar as affected by solution pH, to determine the biochar sorption maximum, and to elucidate the bonding mechanisms that control the solid phase partitioning with biochar. This project is the first phase in a multistage project aimed at sequestering Cu from spent Cu-containing dairy hoofbath waste.

Materials and Methods

Pecan Shell–Based Biochar Production and Characterization

Pecan shells were obtained from Carolina Grains (Lumberton, NC). They were ground using a Retsch Mixer Mill (SR-2000; Cole-Palmer, Vernon Hills, IL) to pass through a 2-mm sieve. Pecan shells were soaked in 1.3 mol L^{-1} KOH in a crucible for 2 h. The use of KOH removes loose organic matter from the pore structure, increasing pore volume, surface area, and possibly reactive surface functional groups (Lima and Marshall, 2005a; Azargohar and Dalai, 2008). The material was then inserted into a Lindberg box programmable furnace equipped with an airtight retort (model 5116HR; Lindberg, Watertown, WI). The furnace retort atmosphere was purged with N_2 using a flow rate of 0.1 m^3 h^{-1}. Pyrolysis occurred by ramping the furnace to 700°C at 5°C min^{-1} and maintaining the temperature for 1 h. Immediately after pyrolysis, the resulting carbonaceous material was steam activated at 800°C for 3 h. Steam was introduced at a flow rate of approximately 2.2 mL min^{-1}. Upon completion of steam activation, the biochar was cooled overnight under a gentle stream of N_2 within the furnace retort. The biochar was then washed with boiling water and rinsed with distilled water until the rinse water reached near neutral pH. The washed sample was dried at 110°C for at least 3 h in a vacuum oven.

Biochar pH was determined in a 1% suspension of biochar in deionized water (Ahmedna et al., 1998); percent ash was determined by dry combustion at 760°C for 6 h; and total C, H, N, and S, and O (by difference) were determined using ASTM Method D 3176 (ASTM, 2006). Biochar total elemental analysis was determined using USEPA Method 3052 (USEPA, 2008). Biochar chemical characteristics are presented in Table 1.

Table 1. Chemical characteristics of potassium hydroxide steam–activated pecan shell–based biochar. All values presented on a dry-weight basis.

Property	KOH steam–activated pecan shell biochar
pH	7.2
Ash, %	10.3
C, %	72.1
H, %	0.55
N, %	0.23
S, %	0.02
O, %	2.5
K, %	11.6
Ca, %	0.60
Mg, mg kg^{-1}	585
Na, mg kg^{-1}	580
Mn, mg kg^{-1}	85
Fe, mg kg^{-1}	37
Al, mg kg^{-1}	71
Cu, mg kg^{-1}	34
Zn, mg kg^{-1}	4.7
Pb, mg kg^{-1}	2.7
Ni, mg kg^{-1}	0.3
Cd, mg kg^{-1}	0.1

To optimize biochar Cu sorption, pH and shaking time effects were examined in a series of studies. First, background solution pH values were adjusted to pH 6 with 0.1 mol L^{-1} potassium hydrogen phthalate and 0.1 mol L^{-1} NaOH or to pH 7, 8, or 9 with 0.1 mol L^{-1} tris(hydroxymethyl) aminomethane and 0.1 mol L^{-1} HCl (Weast, 1985). In triplicate, 1.00 g of biochar and 50 mL of adjusted pH solutions containing 0, 50, 100, 250, and 500 mg L^{-1} Cu (from $CuCl_2{\cdot}2H_2O$) were placed in 50-mL centrifuge tubes and shaken at 120 rpm for 24 h at 20°C. Solutions were then centrifuged, decanted, filtered through a 0.45-μm membrane filter, and analyzed for Cu using inductively coupled plasma optical emission spectroscopy. The amount of Cu sorbed was calculated as the difference between the initial and final solution Cu quantities.

To determine the maximum Cu sorptive capacity of pecan shell–based biochar, the biochar was shaken in pH 6 Cu-containing solutions for 30 d. The pH 6 solution was chosen because biochar sorbed more Cu at pH 6 than at other pH values. Background solution pH was adjusted as previously described. Either 1.00 g of biochar was shaken with solutions containing 0, 50, 100, 250, or 500 mg L^{-1} Cu (from $CuCl_2{\cdot}2H_2O$) or 0.25 g of biochar was shaken with solutions containing 375 or 500 mg L^{-1} Cu. All materials were placed in 50-mL centrifuge tubes and shaken at 120 rpm and 20°C for 30 d. After 30 d, solutions were centrifuged, decanted, filtered through a 0.45-μm membrane filter, and analyzed for Cu using inductively coupled plasma optical emission spectroscopy. The amount of Cu sorbed was calculated from the difference between the initial and final Cu concentrations.

To predict maximum Cu sorption, the data were fitted to the exponential rise equation:

$$Q = a[1 - e^{(bx)}] \qquad [1]$$

where Q is the sorbed biochar Cu (mg kg^{-1}), a is the maximum Cu sorption of biochar (mg kg^{-1}), b is the rate constant for change in Cu sorbed by biochar for a given change in Cu added, and x is the Cu added (mg kg^{-1}).

Biochar Copper Sorption Experiment: Synchrotron Speciation

All biochar solids from the 24-h shaking period were air-dried and analyzed using XAFS spectroscopy to elucidate solid-phase Cu speciation. The XAFS experiments were conducted at the Materials Research Collaborative Access Team's beamline 10-ID, Sector 10 located at the Advanced Photon Source, Argonne National Laboratory, Argonne, Illinois. The electron storage ring operated at 7 GeV in top-up mode. A liquid N_2–cooled, double crystal Si(111) monochromator was used to select incident photon energies, and a platinum-coated mirror was used for harmonic rejection. The monochromator was calibrated by assigning the inflection point of the Kα-absorption edge of Cu metal foil to 8979 eV. The samples were prepared as thin pellets with a hand-operated IR pellet press, and the samples were secured by Kapton tape in sample holders. Five XAS spectra were collected in fluorescence (Lytle detector) and transmission quick-scan mode (0.33 eV steps at 0.1 s integration) at room temperature from −200 to 1000 eV relative to the absorption edge position of Cu. Radiation damage was checked by evaluating successive scans; no damage was observed. Self-absorption was evaluated by comparing transmission and fluorescence spectra. This artifact was only observed in the highest loaded sample (pH 6, 500 mg L^{-1}), and the difference in intensity was small enough that it did not affect data interpretation (peaks in first-derivative XANES were 5 to 11% lower in fluorescence). Thus, to be consistent with the other spectra and to use the best signal-to-noise data, the fluorescence data from this sample were used.

Data processing and linear combination fitting (LCF) of X-ray absorption near-edge structure (XANES) spectra were done with the program Athena (Ravel and Newville, 2005). To determine the Cu speciation in the XANES sample, the following standards were used in the LCF: azurite ($Cu_3(CO_3)_2(OH_2)$), malachite ($Cu_2CO_3(OH)_2$), Cu(II) adsorbed on calcite ($CaCO_3$), Cu(II) adsorbed on Elliot Humic acid (purchased from the International Humic Substances Society), Cu(II)-complexed gluconate (aq), Cu(II)-complexed citrate (aq), Cu(II)-complexed oxalate (aq), Cu(II) acetate salt, $Cu(NO_3)_2$ (aq), $CuSO_4$ (s) (aq), tenorite (CuO), $Cu(OH)_2$ (details of these standard materials are presented in Strawn and Baker [2009]), pseudomalachite ($Cu_5(PO_4)_2(OH)_4{\cdot}H_2O$), liebethenite ($Cu_2(PO_4)OH$), turquoise ($CuAl_6(PO_4)_4(OH)_8{\cdot}4H_2O$), and cornetite ($Cu_3(PO_4)(OH)_3$) (XAFS spectra of these standards were collected during the same beamtime as the Cu incubated biochars). As first pass evaluation criteria, standards were visually inspected to determine which had similar first-derivative XANES spectral peak positions as Cu incubated biochar samples. The standards with peak positions most similar to the biochar samples were used in LCF to determine which combinations best reproduced the XANES spectral features as judged by chi-square statistic, visual inspection of overlaid fits, and percent of standard used in the LCF. Standards that comprised less than 10% in the LCF were not considered in the final fit. This procedure resulted in a base set of standards as follows: Cu–humic acid [HA], azurite, Cu adsorbed on calcite, Cu-gluconate, and CuO. To further reduce the degrees of freedom, Cu-gluconate and Cu adsorbed on calcite were eliminated from the group because they are known to have similar molecular structures as Cu-HA and azurite, respectively. This was confirmed by the similarity in their XANES and extended X-ray absorption fine structure (EXAFS) spectra. The final fitting was done constraining the sum to 1 and not allowing for any shift in energy of standards.

The EXAFS spectra were processed by subtracting a cubic-spline fit between 0.5 and 12.5 Å^{-1} from the background of the normalized spectra. The data were further processed by Fourier transforming using a square window between 1.4 to 10.9 Å^{-1}. The principal component analyses on the chi and XANES spectra (Malinowski, 1977) were done using the program SixPack (Webb, 2005).

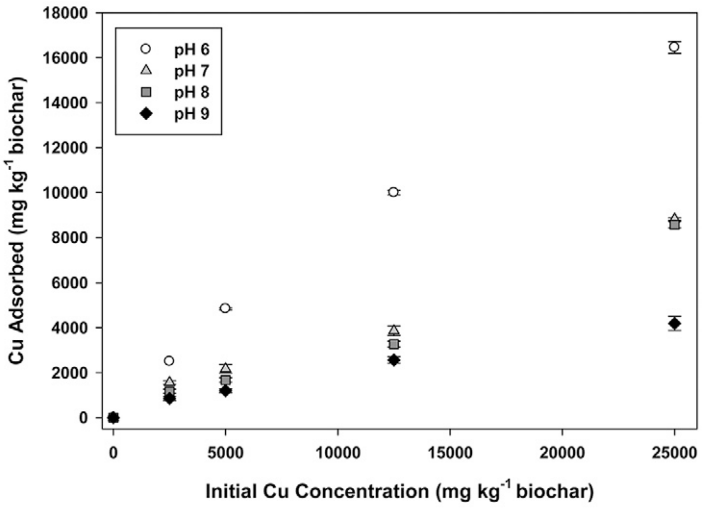

Fig. 1. Effect of solution pH on KOH steam–activated pecan shell biochar to sorb Cu over a 24-h shaking period.

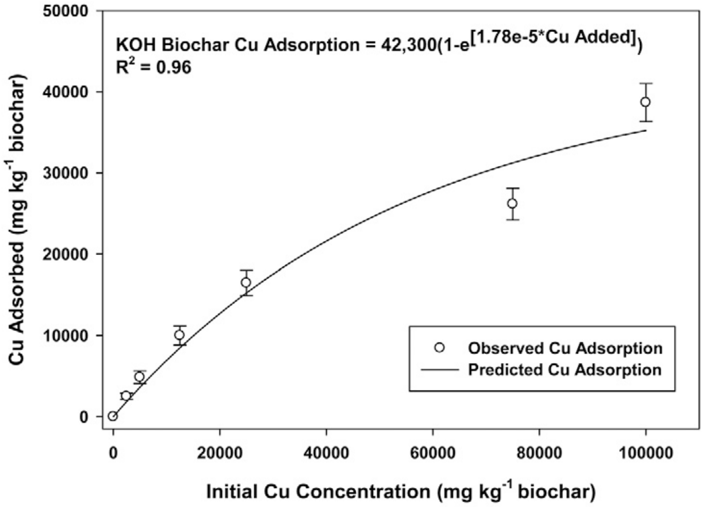

Fig. 2. Potassium hydroxide steam–activated pecan shell biochar Cu sorption maximum, shaken over 30-d period at pH 6.

Results and Discussion

Biochar Copper Sorption at Different Solution pH Values

Biochar sorbed increasing amounts of Cu as the solution pH decreased from 9 to 6 (Fig. 1). At pH 6, carbonyl and hydroxyl functional groups on biochar surfaces may have preferentially bound Cu, whereas at greater pH values precipitation of Cu-hydroxide phases likely occurred. Similar results were reported by Gibert et al. (2005), who studied Cu sorption onto surface functional groups of vegetal compost across a pH gradient. Although a decrease in pH typically would indicate a greater solution metal concentration, Sauvé et al. (2000) compiled data from over 70 different studies and found that only 29% of the variation in soil solution Cu content could be attributed to changes in pH. This was likely due to the influence of dissolved organic phases complexing Cu.

Biochar Copper Sorption Maximum

Copper sorption data on biochar incubated at pH 6 for 30 d (Fig. 2) were fit using Eq. [1]. This model predicted that a maximum of 42,300 mg Cu kg^{-1} (R^2 = 0.96) was sorbed by the KOH steam–activated pecan shell biochar.

Biochar Cu sorption has been studied by other researchers with or without controlling solution pH. Uchimiya et al. (2010a) studied Cu immobilization by poultry broiler litter manure pyrolyzed at 350 and 700°C with or without steam activation and with no control over pH. Copper sorption ranged from 12,600 to 16,400 mg Cu kg^{-1} by biochar that was not steam activated, but steam activation increased the Cu sorption range to 18,400 to 18,500 mg Cu kg^{-1}. The authors explained that steam activation and higher pyrolysis temperatures caused an increase in surface area, which led to greater Cu removal from solution. Lima and Marshall (2005b) found that poultry broiler cake and litter biochars sorbed approximately 28,600 and 22,200 mg Cu kg^{-1} biochar, respectively. These authors buffered the solution pH at 4.8. Lima and Marshall (2005a), however, showed a substantial increase in biochar Cu sorption by adjusting steam flow rates and activation times (pH was not controlled). The authors found that the minimum Cu sorption concentrations ranged from 40,670 to 56,560 mg Cu kg^{-1} biochar when using steam activation at 1 mL min^{-1} for 30 min at 800°C. However, the maximum Cu sorption concentrations were improved to 111,200 to 125,200 mg Cu kg^{-1} biochar after using steam activation at 5 mL min^{-1} for 30 or 45 min and 800°C. Steam activates the biochar by interacting with and removing loose organic matter from the pore structure, effectively increasing pore volume, surface area, and possibly reactive surface functional groups (Lima and Marshall, 2005a) necessary for Cu sorption. In chemical activation, the KOH has a similar effect as steam activation (Azargohar and Dalai, 2008). In our case, Cu sorption was not as great as compared with that of Lima and Marshall (2005a), possibly due to a lower temperature during steam activation or a lower steam flow rate or because the steam activation step had not significantly increased the surface area exposed after the KOH step.

Biochar Copper Sorption Experiment: X-Ray Absorption Fine Structure Speciation

In the XANES spectra from the biochar samples (Fig. 3), the two main peaks between 8980 and 8995 eV arise from the main Cu K-edge (*s* to *p* orbital transition). Because of the Jahn-Teller distortion that occurs in Cu(II), the transition energies to the p_{xy} and p_z orbitals were different, thus creating the two energy transitions on the Cu K-edge. The peak centered at approximately 8985 eV is due to the p_z orbital transition. The energy of *s* to p_z orbital transition is sensitive to molecular coordination and thus can be used to monitor changes in molecular structure. The XANES spectra from the biochar samples were very similar but not exactly the same. The subtle differences within each pH group and between groups indicate some changes in the average molecular structure between samples. The changes were due to distinct distributions of Cu species in the samples. Within the pH groups, the most significant differences occur in the pH 6 incubated samples. In this group, the amplitude of the peak at 8985.4 eV was inversely related to loading level (the trend was the same in the transmission data [not shown]). Further, in the pH 6 samples, the main edge peaks at 8985.4 eV were 0.8 eV greater than the same peak in the samples incubated at pH 7, 8, and 9, suggesting the average molecular environment of sorbed Cu in the samples incubated at pH 6 was distinct.

Peak positions in Cu(II) XANES spectra are distinct for different molecular compounds (Supplemental Fig. S1) and thus can be used for qualitative identification of Cu species. Samples that have multiple types of reaction surfaces, such as biochar, can have more than one species present. Principle component analysis conducted on the XANES spectra suggested that there are five components; however, three components account for 95% of the variance in the XANES, suggesting that the other two components were minor. Linear combination fitting can be used to quantify the amount of each species. Error for LCF is generally 10 to 20% absolute due to the fact that the peak positions and intensities of some of the standard XANES spectra are similar. Percent of each standard fit indicates the amount of a particular species likely in the sample. Figure 4 shows best and worst LCF of XANES for two biochar samples. The biochar sample incubated at pH 6 with 50 mg L^{-1} Cu was fit using the standards Cu adsorbed on HA (66%), tenorite (14%), and azurite (20%). This suggests that the Cu in the biochar was coordinated in a molecular structure similar to Cu in those three standards. Copper adsorption on HA has been shown to be predominantly a five-membered ring ligand structure (Karlsson et al., 2006; Strawn and Baker, 2009; Manceau and Matynia, 2010), and this structure is a common coordination moiety for many Cu-ligands (e.g., Cu glutamate) (Fitts et al., 1999; Manceau and Matynia, 2010). Thus, the Cu K-edge XANES indicated that Cu in the biochar at pH 6 occurred predominantly in a molecular structure similar to Cu complexed on HA, which is a bidentate, five-member ring structure involving carboxyl and amine functional groups.

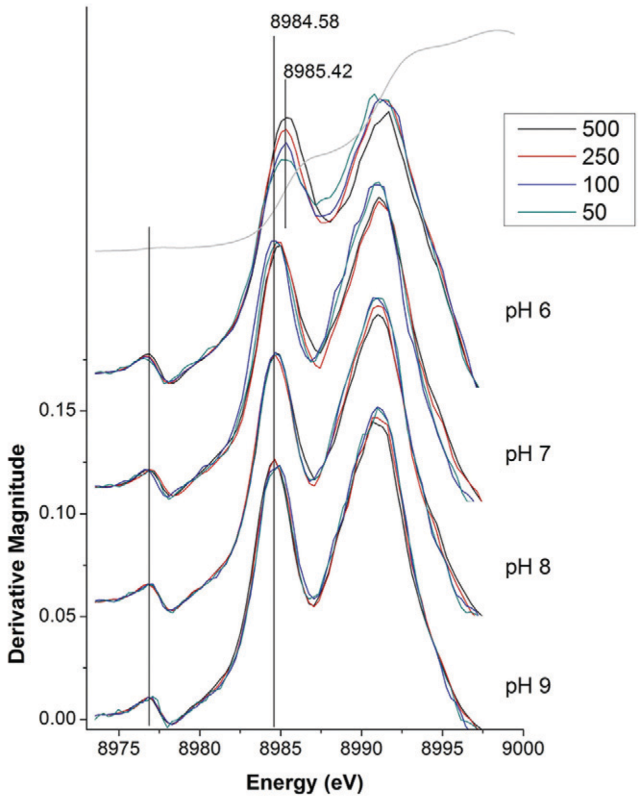

Fig. 3. First derivative of X-ray absorption near edge structure spectra for biochar incubated at different pH and concentrations. One nonderivate spectra (gray) is overlaid for reference. Vertical lines are placed on peaks to allow energy comparison between spectra.

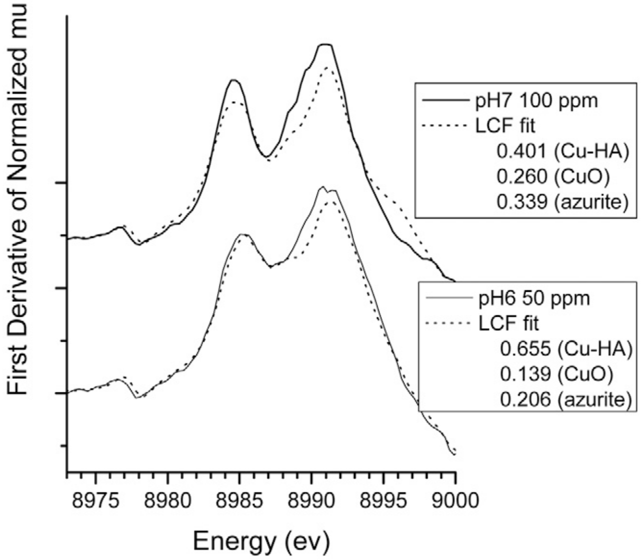

Fig. 4. First-derivative X-ray absorption near-edge structure spectra from biochar samples with highest and lowest fit statistic (Table 2) compared with linear combination fitting (LCF) results.

The LCF results of the XANES from the 16 biochar samples incubated under different pH and Cu concentrations are presented in Table 2. The fraction of HA fit in the first derivative XANES spectra was negatively correlated to pH, although it was not necessarily linear (Supplemental Fig. S2). The remainder of the LCF components was split between azurite and tenorite, with azurite taking a slightly larger role. For example, for the sample incubated at pH 9 with 500 mg L^{-1} Cu, 38% was fit with azurite, 28% was fit with tenorite, and 35% was fit with Cu adsorbed to HA (i.e., Cu in a five-membered ring ligand complex).

Additional support of the molecular structure of Cu on biochar was inferred by analyzing the EXAFS spectra. The EXAFS spectral features of Cu sorbed on biochar were dominated by O backscattering, with some weak features indicative of second shell backscatterers (Supplemental Fig. S3).

Principal component analysis of the chi spectra showed a minimum of the empirical indicator function at three components (Eigenvectors), which account for 84% of the variance in the 16 spectra.

Both EXAFS and XANES spectra suggest that there are at least three unique Cu species in the 16 spectra from the biochar samples. Thus, molecular modeling to derive the theoretical structure of Cu is limited to first-shell interpretations of average bond distance. Reproducing the EXAFS spectra using the three standards at the same proportions as the XANES LCF results had a larger residual than if the LCF was optimized on the EXAFS data. This is not uncommon because, compared with XANES, EXAFS is more sensitive to structural disorder and data processing differences, which cannot be consistently accounted for between the unknowns and standards. However, analysis of Fourier transforms (FT) to isolate individual frequencies in the chi, which are indicative of backscattering pairs of atoms, and comparison to FT from standard spectra provide qualitative information about average molecular structures.

The average atomic distances between the central Cu atom and surrounding O atoms is represented by the first large peak position in the FT, which is approximately 0.44 Å less than the true atomic distances (based on the first O coordination shell in CuO and Cu adsorbed on humic acid). The principal component analysis of the chi spectra indicated that there were three components that explain most of the variability between the 16 spectra. This was also observed visually in the FT plots (Supplemental Fig. S4). That is, the 16 FT of the biochar chi data can be grouped into three categories based on peak positions. The best representatives of the three FT groups based on uniqueness of peak positions and data quality are the pH 9 250 mg L^{-1}, the pH 9 500 mg L^{-1}, and the pH 6 50 mg L^{-1} incubated samples (Fig. 5). At pH 6, the peak at 1.48 Å in the FT was in line with the first-shell peak in Cu adsorbed on HA. Based on this, it appears that at lower pH, the Cu exists in a molecular environment similar to the Cu adsorbed on the model HA standard. In the samples incubated at pH 7, 8, and 9, the first-shell peak position in the FT increases to 1.51 Å, corresponding to an increase in the average Cu-O atomic distance, consistent with Cu oxides and carbonates. The second shell peaks between 2.01 and 2.08 Å were also consistent with trends showing that as pH and loading level increased, carbonate and oxide phases in the sample also increased. Thus, the molecular speciation results from the qualitative EXAFS spectral analysis of the Cu adsorbed on the biochar are in agreement with the results from the XANES data analysis.

The XANES and EXAFS spectra analysis show that sequestration of Cu by biochar results in three different Cu species. The distribution between the three species was pH and concentration dependent. Based on the adsorption behavior and the XAFS data, we interpreted the pH-dependent sorption mechanisms of Cu on the biochar as follows: at low pH the Cu was predominantly sorbed onto the organic functional groups present on biochar

Table 2. Linear combination fitting results of X-ray absorption near-edge structure for Cu sorbed to biochar using Cu sorbed on humic acid, tenorite, and azurite standards.

Cu concentration	pH	Humic acid	Tenorite	Azurite	*R* factor†
			Fraction fit		
500	9	0.35	0.27	0.38	0.0166
250	9	0.37	0.24	0.39	0.0174
100	9	0.40	0.21	0.39	0.0212
50	9	0.40	0.22	0.37	0.0216
500	8	0.42	0.22	0.36	0.0101
250	8	0.39	0.24	0.37	0.0162
100	8	0.40	0.21	0.38	0.0218
50	8	0.41	0.20	0.38	0.0231
500	7	0.48	0.17	0.34	0.0061
250	7	0.45	0.16	0.38	0.0094
100	7	0.40	0.26	0.34	0.0236
50	7	0.44	0.20	0.37	0.0208
500	6	0.62	0.09	0.29	0.0080
250	6	0.62	0.09	0.29	0.0045
100	6	0.64	0.10	0.26	0.0050
50	6	0.66	0.14	0.21	0.0038

† (sum (data-fit)^2)/(sum data^2) (Ravel and Newville, 2005).

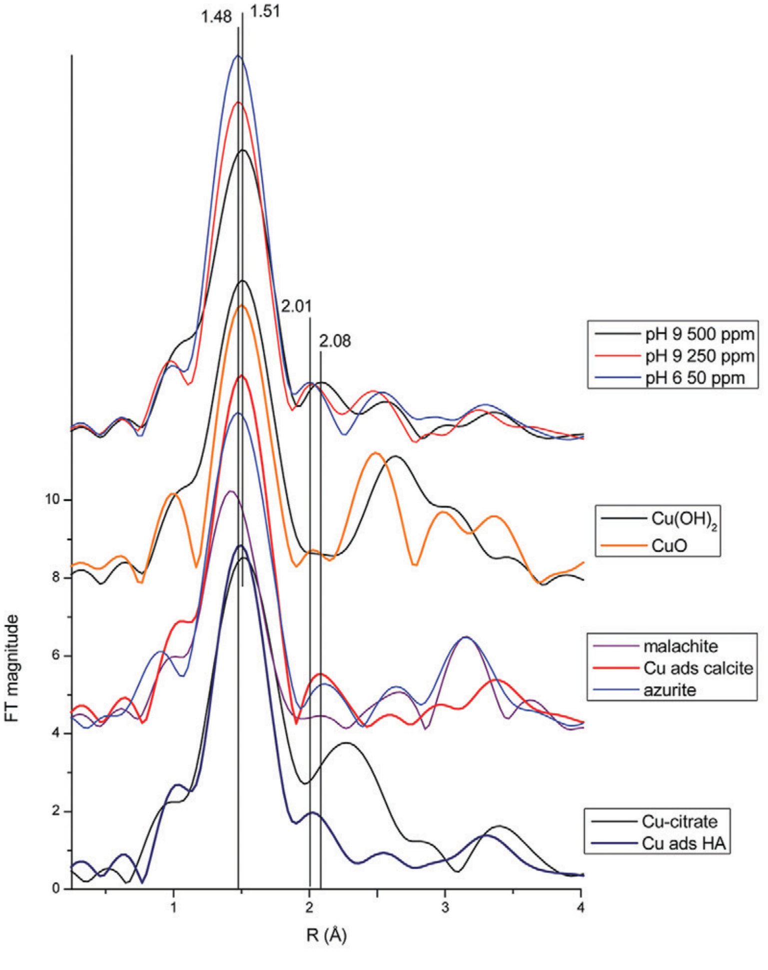

Fig. 5. Fourier transforms (FT) of thee biochar samples incubated with Cu and representative Cu standards. Δk = 1.4 –10.9 Å^{-1}.

surfaces; as pH increased, mineral precipitation may be coating biochar surfaces and blocking pores, making the organic functional groups unavailable and leading to decreased Cu adsorption. These findings suggest that at lower solution pH values (e.g., waters generated from acid mine drainage), Cu sorption on biochar may be an important remediation option.

Summary

The ability of KOH steam–activated pecan shell biochar to sorb solution Cu was investigated across a pH range, the Cu sorption maximum was calculated, and speciation was determined using XAS. Findings showed that, over a 24-h period, as solution pH was decreased from 9 to 6, biochar removed greater quantities of Cu (from ~4,000 to 16,000 mg Cu kg^{-1} sorbed). The XAS results showed that at pH 6, Cu was predominantly bound to biochar organic functional groups, with lesser amounts precipitated as CuO or $CuCO_3$. At pH 7, 8, and 9, CuO or $CuCO_3$ precipitation on the biochar increased. After a 1-mo shaking period in pH 6 solution, the biochar sorption maximum was 42,300 mg kg^{-1}. These research findings suggest that biochars could be used to remove Cu from water in industrial and environmental applications. However, understanding the mechanisms behind how a particular biochar reacts within ecosystems is paramount for designing best management strategies that use biochar for Cu removal.

References

Ahmedna, M., W.E. Marshall, and R.M. Rao. 2000. Production of granular activated carbon from select agricultural by-products and evaluation of their physical, chemical, and adsorption properties. Bioresour. Technol. 71:113–123. doi:10.1016/S0960-8524(99)00070-X

ASTM. 2006. Petroleum products, lubricants, and fossil fuels: Gaseous fuels; coal and coke. ASTM Inter., West Conshohocken, PA.

Azargohar, R., and A.K. Dalai. 2008. Steam and KOH activation of biochar: Experimental and modeling studies. Microporous Mesoporous Mater. 110:413–421. doi:10.1016/j.micromeso.2007.06.047

Beesley, L., E. Moreno-Jimenez, and J.L. Gomez-Eyles. 2010. Effects of biochar and greenwaste compost amendments on mobility, bioavailability and toxicity of inorganic and organic contaminants in a multi-element polluted soil. Environ. Pollut. 158:2282–2287. doi:10.1016/j.envpol.2010.02.003

Fitts, J.P., P. Persson, G.E. Brown, Jr., and G.A. Parks. 1999. Structure and bonding of Cu(II) glutamate complexes at the γ-Al_2O_3–water interface. J. Colloid Interface Sci. 220:133–147. doi:10.1006/jcis.1999.6521

Gibert, O., J. de Pablo, J.L. Cortina, and C. Ayora. 2005. Sorption studies of Zn(II) and Cu(II) onto vegetal compost used on reactive mixtures for in situ treatment of acid mine drainage. Water Res. 39:2827–2838. doi:10.1016/j.watres.2005.04.056

Hartley, W., N.M. Dickinson, P. Riby, and N.W. Lepp. 2009. Arsenic mobility in brownfield soils amended with green waste compost or biochar and planted with *Miscanthus*. Environ. Pollut. 157:2654–2662. doi:10.1016/j.envpol.2009.05.011

Hua, L., W. Wu, Y. Liu, M.B. McBride, and Y. Chen. 2009. Reduction of nitrogen loss and Cu and Zn mobility during sludge composting with bamboo charcoal amendment. Environ. Sci. Pollut. Res. 16:1–9. doi:10.1007/s11356-008-0041-0

Ippolito, J.A., T. Ducey, and D. Tarkalson. 2010. Copper impacts on corn, soil extractability, and the soil bacterial community. Soil Sci. 175:586–592. doi:10.1097/SS.0b013e3181fe2960

Lima, I.M., and W.E. Marshall. 2005a. Adsorption of selected environmentally important metals by poultry manure-based granular activated carbons. J. Chem. Technol. Biotechnol. 80:1054–1061. doi:10.1002/jctb.1283

Lima, I.M., and W.E. Marshall. 2005b. Granular activated carbons from broiler manure: Physical, chemical and adsorptive properties. Bioresour. Technol. 96:699–706. doi:10.1016/j.biortech.2004.06.021

Lima, I.M., and W.E. Marshall. 2005c. Utilization of turkey manure as granular activated carbon: Physical, chemical and adsorptive properties. Waste Manag. 25:726–732. doi:10.1016/j.wasman.2004.12.019

Low, K.S., C.K. Lee, and S.C. Liew. 2000. Sorption of cadmium and lead from aqueous solutions by spent grain. Process Biochem. 36:59–64. doi:10.1016/S0032-9592(00)00177-1

Kalis, E.J.J., E.J.M. Temminghoff, L. Weng, and W.H. van Riemsdijk. 2006. Effects of humic acid and competing cations on metal uptake by *Lolium Perenne*. Environ. Toxicol. Chem. 25:702–711. doi:10.1897/04-576R.1

Karlsson, T., P. Persson, and U. Skyllberg. 2006. Complexation of copper(II) in organic soils and in dissolved organic matter: EXAFS evidence for chelate ring structures. Environ. Sci. Technol. 40:2623–2628. doi:10.1021/es052211f

Malinowski, E.R. 1977. Determination of the number of factors and the experimental error in a data matrix. Anal. Chem. 49:612–617. doi:10.1021/ac50012a027

Manceau, A., and A. Matynia. 2010. The nature of Cu bonding to natural organic matter. Geochim. Cosmochim. Acta 74:2556–2580. doi:10.1016/j.gca.2010.01.027

McBride, M.B., and J.J. Blasiak. 1979. Zinc and copper solubility as a function of pH in an acid soil. Soil Sci. Soc. Am. J. 43:866–870. doi:10.2136/sssaj1979.03615995004300050009x

Özer, A., D. Özer, and A. Özer. 2004. The adsorption of copper(II) ions on to dehydrated wheat bran (DWB): Determination of the equilibrium and thermodynamic parameters. Process Biochem. 39:2183–2191. doi:10.1016/j.procbio.2003.11.008

Ravel, B., and M. Newville. 2005. ATHENA, ARTEMIS, HEPHAESTUS: Data analysis for X-ray absorption spectroscopy using IFEFFIT. J. Synchrotron Radiat. 12:537–541. doi:10.1107/S0909049505012719

Rodriguez-Rubio, P., E. Morillo, L. Madrid, T. Undabeytia, and C. Maqueda. 2003. Retention of copper by a calcareous soil and its textural fractions: Influence of amendment with two agroindustrial residues. Eur. J. Soil Sci. 54:401–409. doi:10.1046/j.1365-2389.2003.00529.x

Sauvé, S., W. Hendershot, and H.E. Allen. 2000. Solid-solution partitioning of metals in contaminated soils: Dependence of pH, total metal burden, and organic matter. Environ. Sci. Technol. 34:1125–1131. doi:10.1021/es9907764

Stehouwer, R., and G. Roth. 2009. Copper sulfate hoof baths and copper toxicity in soil. Available at http://www.das.psu.edu/news/dd200403-03 (verified 9 Sept. 2011).

Strawn, D.G., and L.L. Baker. 2009. Molecular characterization of copper in soils using X-ray absorption spectroscopy. Environ. Pollut. 157:2813–2821. doi:10.1016/j.envpol.2009.04.018

Uchimiya, M., I.M. Lima, K.T. Klasson, S. Chang, L.H. Wartelle, and J.E. Rodgers. 2010a. Immobilization of heavy metal ions (Cu^{II}, Cd^{II}, Ni^{II,} and Pb^{II}) by broiler litter-derived biochars in water and soil. J. Agric. Food Chem. 58:5538–5544. doi:10.1021/jf9044217

Uchimiya, M., I.M. Lima, K.T. Klasson, and L.H. Wartelle. 2010b. Contaminant immobilization and nutrient release by biochar soil amendment: Roles of natural organic matter. Chemosphere 80:935–940. doi:10.1016/j.chemosphere.2010.05.020

USEPA. 2008. Microwave assisted acid digestion of siliceous and organically based matrices. *In* Test methods for evaluating solid waste, physical/chemical methods. SW-846. USEPA, Washington, DC. Available at http://www.epa.gov/osw/hazard/testmethods/sw846/pdfs/3052.pdf (verified 9 Sept. 2011).

Weast, R. (ed.) 1985. CRC handbook of chemistry and physics. 65th ed. CRC Press, Boca Raton, FL.

Webb, S.M. 2005. Sixpack: A graphical user interface for XAS analysis using IFEFFIT. Phys. Scr. T 115:1011–1014. doi:10.1238/Physica.Topical.115a01011

Xia, K., W. Bleam, and P.A. Helmke. 1997. Studies of the nature of Cu^{2+} and Pb^{2+} binding sites in soil humic substances using X-ray absorption spectroscopy. Geochim. Cosmochim. Acta 61:2211–2221. doi:10.1016/S0016-7037(97)00079-3